Kinetic-energy- and angular-resolved fragmentation of CO in vibrational-resolved C 1*s* excitation

Norio Saito,[1] Franz Heiser,[2] Oliver Hemmers,[2,*] Kornel Wieliczek,[2]
Jens Viefhaus,[2] and Uwe Becker[2]
[1]*Electrotechnical Laboratory, 1-1-4 Umezono, Tsukuba-shi, Ibaraki 305, Japan*
[2]*Fritz-Haber-Institut der Max-Planck-Gesellschaft, Faradayweg 4-6, D-14195 Berlin, Germany*
(Received 4 March 1996)

Angular distributions of $C^+ + O^+$ from CO were measured, following vibrationally resolved C 1*s* excitations into the $2p\pi$, $3s\sigma$, and $3p\pi$ orbitals as well as into higher unresolved orbitals. A time-of-flight mass spectrometer, with a multihit-type position-sensitive anode, was used for the measurements. The anisotropy parameters (β) of $C^+ + O^+$ approach their theoretically expected values as the released kinetic energy in the fragmentation increases. The value of the β parameters remains constant for all vibrational states within each orbital. [S1050-2947(96)06409-8]

PACS number(s): 33.80.Gj, 33.80.Eh, 33.80.Rv

I. INTRODUCTION

Inner-shell photoabsorption spectra of unsaturated diatomic molecules are characterized by two kinds of resonances (π^* and σ^*) and by transitions to Rydberg orbitals [1]. To investigate these excited electronic states, angular distributions of fragment ions were recently measured for N_2 [2–6], CO [7–9], O_2 [6,10,11], and NO [12,13] using linear polarized monochromatic soft x rays. When the bond rupture of the core excited or ionized molecules occurs in time scales shorter than that of the molecular rotation, anisotropic distributions of fragment ions reflect the orientations of the molecular bond axis, at the moment of the initial electronic excitation. The angular distribution of fragment ions is therefore expressed by the following equation in the dipole approximation:

$$\frac{d\sigma}{d\Omega} = \frac{\sigma_t}{4\pi}[1 + \beta P_2(\cos\theta)], \tag{1}$$

where $P_2(\cos\theta) = (3\cos^2\theta - 1)/2$ is the second-order Legendre polynomial, θ is the angle between the electric field vector and the velocity vector of the fragment ion, σ_t is the total cross section, and β is the angular distribution parameter [14]. When a molecule is excited from a Σ state to a Σ state by linear polarized light, the molecule is oriented preferentially parallel to the electric field vector of the light, yielding a β parameter of 2. For a Σ-to-Π transition, the molecule is oriented preferentially perpendicular to the electric field vector, approaching a β of -1 for the pure transition. The case of isotropic fragmentation is characterized by a β value of 0. One can therefore conclude that angular distribution measurements are a direct method for determining the symmetry of inner-shell excited states of diatomic molecules.

Two different techniques were used to obtain previous angular distribution measurements. (1) Ion time-of-flight (TOF) spectra were measured with the axis of the flight tube oriented at 0°, 90°, and 54.7° with respect to the polarization vector of the incident soft x rays and the β values determined by deconvolution of the shapes of the ion signal peaks [2,3,9,10,12]. (2) The total ion current was measured at several angles, either simultaneously or sequentially, to determine the angular dependence of the flux of the fragmentations [4–8,11,13]. Method (1) can resolve the mass-to-charge ratios of ions and their kinetic energies but the uncertainty in β is greater than that of method (2). Method (2) can resolve neither the mass-to-charge ratios nor the kinetic energies of the fragment ions. Ions with low kinetic energies were, however, discriminated by applied reverse fields. To our knowledge, mass-to-charge ratio-resolved and kinetic-energy-resolved angular distribution measurements have not been previously reported.

Theoretically in a 1*s* to π^* ($\Sigma \rightarrow \Pi$) excitation, the angular distribution of fragment ions should have a β value of -1. However, all previously reported β values at the π^* excitation, with the exception of Lee *et al.* [6], are in the range of -0.7 to -0.95 [2–13]. It is not clear if these differences were caused by the long lifetime of core hole states, the long lifetime of intermediate states after core hole decay, or other experimental uncertainties.

Vibrational structures of core excited molecular valence and Rydberg states became a subject of interest after a high-resolution soft-x-ray monochromator became available, allowing for the study of absorption spectra of CO in the C 1*s* excitation region [15–17]. The results validated the equivalent core model, which considers the electronic structure of a core excited molecule (CO, N_2) as being equivalent to that of the corresponding valence excited molecule with a nuclear charge of $Z+1$ (NO) [16,18]. A discrepancy exists between the absorption spectra of CO and N_2. For CO, none of the $ns\sigma$ states with $n>3$ of CO are visible, whereas these states are clearly exhibited in the N_2 excitation spectrum. The assignments made by Chen *et al.* [18] in the absorption spectrum of the N 1*s* excitations give rise to an anomaly in

*Present address: Department of Chemistry, University of Nevada, Las Vegas, NV 89154-4003.

the oscillator strengths across the $ns\sigma$ Rydberg series where the $4s\sigma$ transition (peak 6 [18]) is stronger than the $3s\sigma$ transition. The symmetry-resolved ion yield spectrum of N_2 in the N $1s$ Rydberg region indicates that there are intensities for both σ-type and π-type transitions at peak 6 in Ref. [18]. This peak is comprised of transitions from N $1s$ to $4s\sigma$ and $3d\pi$, two nearly degenerate Rydberg states [19]. In Ref. [19], it is also implied that $ns\sigma$ states exist in the CO C $1s$ excitation spectrum. This suggests that the equivalent core model is not complete. Ion yield spectra in the C $1s$ excitation region have been measured with vibrational resolution, showing that the vibrational levels of final Rydberg states become selectively depopulated. This is due to the interaction with dissociative decay channels, leading to ionic fragmentation and the missing $4s\sigma$ series becoming apparent [20]. To determine the symmetry of the Rydberg excitation states for further consideration of the assignments, it is important to measure the angular distribution of ions in the vibrational-resolved C $1s$ excitation region.

This paper reports on β values and their kinetic-energy dependence for $C^+ + O^+$ fragmentation from CO following C $1s$ excitation. These results were obtained on a modified SX700 soft-x-ray monochromator, which resolved core vibration levels, and a newly developed angle-resolved time-of-flight mass spectrometer with a position-sensitive detector.

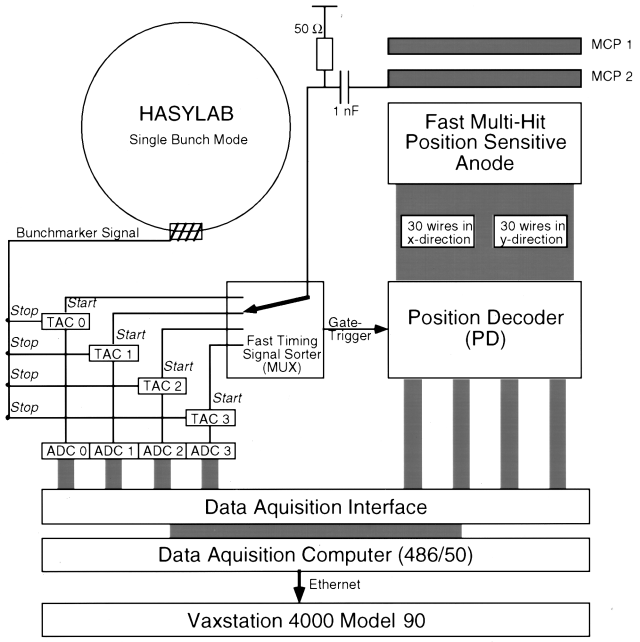

FIG. 1. Angle-resolved time-of-flight ion spectrometer with a position-sensitive anode including the electronic setup for data registration.

II. EXPERIMENT

The experiments were performed at beamline BW3 of the Hamburger Synchrotronstrahlungslabor (HASYLAB) of DESY [21]. This beamline is a triple N-pole undulator beamline ($N=21,33,44$) equipped with a high-resolution SX700 plane grating monochromator modified for high photon throughput. This instrument has a routinely achievable resolution of 3000 with a photon flux of 10^{12} photons/sec. The degree of linear polarization of the light was determined to be 98% at 300 eV by measuring the angular distributions of the Ne $2s$ and $2p$ photoelectrons. Angular distributions of fragment ion pairs were measured with a newly developed TOF mass spectrometer, comprised of a McLaren-type space-charge-focusing instrument of 42 mm length and a multihit anode as shown in Fig. 1 [22]. The spectrometer was positioned at an angle of 55° with respect to the electric field vector of the photon beam. The partial CO pressure was lower than 3×10^{-6} mbar. The ions were detected by microchannel plates (MCP's) with a position-sensitive anode, consisting of 30×30 wires with 0.5 mm spacing. The voltages on the pusher, the extractor, the drift tube, the surface of the MCP, and the anode were 800, -800, -1605, -3752, and 0 V, respectively, to satisfy the required space-focusing condition. The TOF of the ions was measured with respect to the bunch marker of the storage ring, which was operated in the single-bunch or double-bunch modes with time windows of 964 or 482 nsec, respectively. The electronic setup used to detect TOF and ion positions is illustrated in Fig. 1. The pulses from the end of the second MCP were utilized to determine the ion TOF and timing signals for the position decoder. Since the pulses from the second MCP were positive, these pulses were inverted in order to fit the NIM standard. Following this inversion, ion signals were selected by a fast timing signal sorter (multiplexer) placing them into first, second, third, and fourth positions. Each selected signal was channeled into the start connector of a time-to-amplitude converter (TAC). The stop pulse for all TAC's was provided from the bunch marker of the ring. The TAC signals were put into analog-to-digital converters (ADC's) and from there transferred into a 486 personal computer. When two ions were detected at the anode in a given time window, the TOF and the position signal on the anode for each pair of ions were recorded in the personal computer.

The upper part of Fig. 2 shows the time information of two coincident ion events at a photon energy of 287.4 eV, which corresponds to the C $1s\rightarrow2p\pi$ excitation in CO. The x axis is the TOF of the first detected ion and the y axis the TOF of the second detected ion. The coincidence signal of $C^+ + O^+$ is the most intense, but we can also see the weak coincidence maps of $C^+ + O^{2+}$, $C^{2+} + O^+$, and $C^{2+} + O^{2+}$. These coincidences point downwards on the right-hand side. The maps pointing upwards on the right-hand side are generated from false coincidences. The lower left-hand side of Fig. 2 shows positions of the first arrival and second arrival ions, which correspond to C^+ and O^+ ions, respectively. The unit of the x and y axes is the channel number, and one channel corresponds to 0.5 mm. The ions were spread out over 5 mm because of their kinetic-energy distribution. With this data we can determine the original orientation and kinetic-energy release of the dissociating molecule using the following equation:

$$p^2=\left[\frac{d}{\frac{T_1}{m_1}+\frac{T_2}{m_2}}\right]^2+\left[\frac{E}{\frac{1}{q_1}+\frac{1}{q_2}}\right]^2\{(T_1-T_2)-(T_{01}-T_{02})\},$$

$$\theta=\cos^{-1}\left[\frac{d}{p\left(\frac{T_1}{m_1}+\frac{T_2}{m_2}\right)}\right], \tag{2}$$

where p and θ denote the momentum and the angle between the molecular axis and the electric field vector of the photon beam, respectively. $T_{1,2}$, $T_{01,02}$, $q_{1,2}$, and $m_{1,2}$ represent the flight time, the flight time for zero kinetic energy, the electric charge, and mass of the first detected ions and the second detected ions, respectively. Here, d is the distance between the first detected ion and the second detected ion on the anode and E is the electric field in the collision region. In Eq. (2), the momentum conservation law is adopted and it gives the momentum vector for each event. The summation of the momentum vectors of all events in steps of 10° for the angular distribution and in steps of 0.1 eV for the total kinetic energy creates a three-dimensional image of the process. The lower right-hand side of Fig. 2 shows the three-dimensional representation of the angular distribution for $C^+ + O^+$ ion pairs with total kinetic energies between 12 and 18 eV. The electric field vector of the incident light is the horizontal direction as shown in the figure. This three-dimensional figure suggests that the fragmentation of $C^+ + O^+$ occurs preferentially perpendicular to the electric field vector at the C $1s \rightarrow 2p\pi$ excitation. In order to derive the β parameter, the three-dimensional image is fitted to the following three-dimensional cross-section distribution using a least-square method:

$$\frac{d\sigma}{d\Omega}=\frac{\sigma_t}{4\pi}\left[1-\frac{\beta}{2}+\frac{3\beta}{4}\{(1+P)\cos^2 a+(1-P)\cos^2 b\}\right]. \tag{3}$$

P denotes the degree of linear polarization of the incident light, a indicates the angle between the direction of fragmentation and the direction of polarization of the light, and b is the angle between the direction of fragmentation and the direction perpendicular to the direction of polarization [23]. The fitting procedure applied for the three-dimensional representation in Fig. 2 results in the β value of -0.86.

III. KINETIC-ENERGY RELEASE DISTRIBUTIONS IN $C^+ + O^+$ FRAGMENTATION

Figure 3 shows the kinetic-energy release distributions (KERD's) of C^+-O^+ fragmentation at a photon energy of 287.4 eV, which corresponds to the transition of CO C $1s$ to the $2p\pi(\nu=0)$ unoccupied orbital (solid curve). The dotted curve is obtained from analysis of photoion-photoion coincidence spectra of $C^+ + O^+$, yielding peak energies of 8.5, 12.5, and 16.0 eV full width at half maximum (FWHM) of 4.0, 3.0, and 10.0 eV, and weight of 1.0, 0.2, and 0.5, respectively, measured at 287 eV [24]. The present KERD has its maximum at about 7.5 eV and a broad shape. However, the KERD by Hitchcock *et al.* shows the maximum at 8.5 eV and a narrower shape than that of the present curve. The broadness of the present KERD is caused by the energy resolution of our experiment (1.5 eV), which is limited by the position resolution and the fields applied in the TOF mass spectrometer.

TABLE I. The β parameters of diatomic molecules at the $1s \rightarrow \pi^*$ excitations measured previously.

Molecules (inner shell)	β parameter	Reference
N_2 (N $1s$)	-0.71 ± 0.15	2
	-0.88 ± 0.05	3
	-0.9	5
	-1.0	6
CO (C $1s$)	-0.95 ± 0.05	8
	-0.79 ± 0.2	9
O_2 (O $1s$)	-0.89 ± 0.15	10
	-1.0	6
NO (N $1s$)	-0.75 ± 0.2	12

All the KERD's at other photon energies were similar to the KERD in Fig. 3, which shows that the intermediate states which produce $C^+ + O^+$ do not change substantially with the initial core excited states. The initial state of $CO^*(1s^{-1}2p\pi)$ usually deexcites into CO^+ through participator- or spectator-type Auger transitions. The CO^+ mainly remains as a singly charged molecular ion or dissociates into $C^+ + O$. The fragmentation of $C^+ + O^+$ occurs from CO^{2+}, created from deexcitation processes such as double Auger transitions or spectator-type Auger transitions involving inner valence electrons followed by second-step autoionization. The initial state of $CO^+(1s^{-1})$ mainly decays through Auger transitions, producing CO^{2+}, which primarily dissociates into $C^+ + O^+$. The decay of double charged cation CO^{2+} fragments into $C^+ + O^+$ occurs regardless of the initial state.

The dissociation processes of CO^{2+} into $C^+ + O^+$ have been discussed in detail by Hitchcock *et al.* [24]. Wetmore *et al.* [25] calculated the dissociative CO^{2+} curves leading to C^+-O^+. Findings from these studies along with dissociation pathway show that kinetic energies around 7.5 eV are mainly produced from the following pathway:

$$CO^{2+}(^3\Sigma^-, 43.4 \text{ eV}) \rightarrow C^+(^2P) + O^+(^4S) + 7.4 \text{ eV}. \tag{4}$$

IV. KINETIC-ENERGY DEPENDENCE OF THE β PARAMETER OBSERVED IN THE $C^+ + O^+$ FRAGMENTATIONS

In many previous studies, the value of the β parameter of the π^* excitations in diatomic molecules did not reach the theoretically expected value, -1. Table I lists the β parameters of N_2 [2,3,5,6], CO [8,9], O_2 [6,10], and NO [12] measured at their corresponding $1s \rightarrow \pi^*$ excitation. Since some studies on angular distributions of fragment ions did not evaluate concrete β values, [7,11,13] the list in Table I does not cover all the references. The β values are in the range of -0.7 to -0.95, except the values for N_2 and O_2 by Lee *et al.* [6]. Theoretically, when exciting a $1s$ electron to the π^* orbital by linear polarized photons, the molecular axis is preferentially oriented perpendicular to the electric

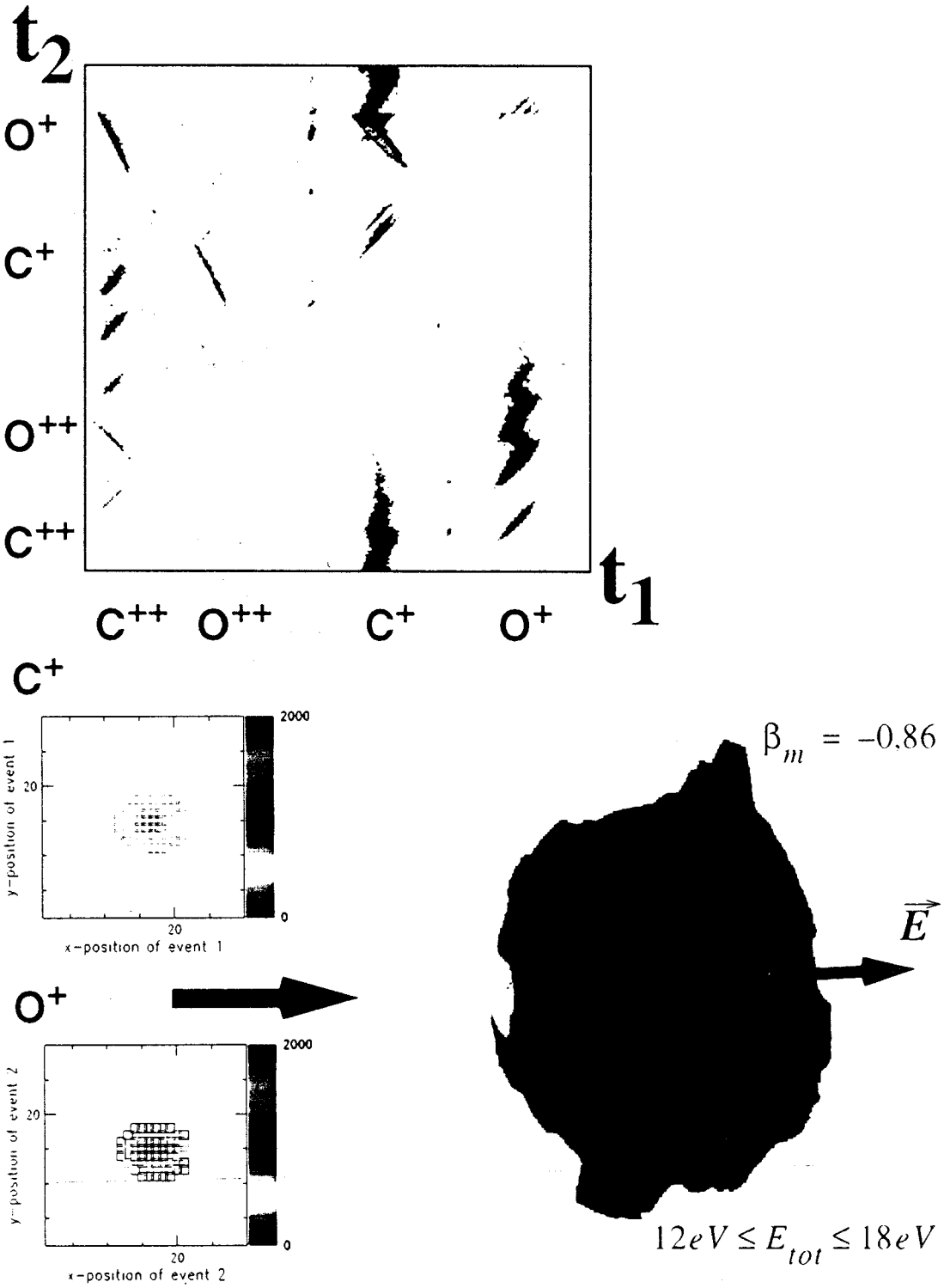

FIG. 2. Top: coincidence map of the flight time of the first and second detected ions. Lower left: position of the first and the second detected ions on the MCP, which correspond to C^+ and O^+ ions, respectively. Lower right: three-dimensional representation of the angular distribution for $C^+ + O^+$ ion pairs with total kinetic energies between 13 and 18 eV.

field vector of the photons. Since the rotational motion of the molecules is much slower than their fragmentation, the direction of fragmentation is in the same direction as the initial molecular bond axis, which would result in a β parameter of -1. Some proposed reasons for the deviations in the β values are the long lifetime of core hole states, the long lifetime of the intermediate states after core hole decay, or specific experimental problems. Since the lifetime of the C $1s$ and O $1s$ core holes in CO are on the order of 10^{-14} s [26,27], and the period of the molecular rotation for CO is on the order of 10^{-12} s [28], the long lifetime of the core hole should not affect the β parameter. Hemmers *et al.* [8] have obtained a β value of -0.95 for CO detecting only fast ionic fragments, which is close to -1. The β values obtained by other au-

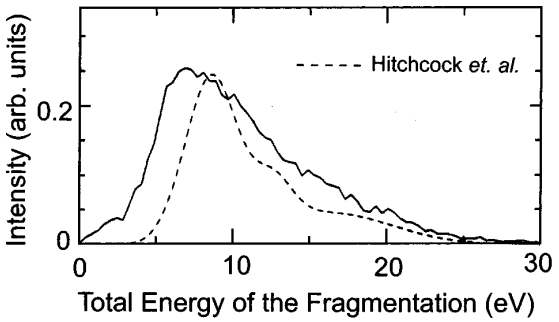

FIG. 3. Kinetic-energy release distributions of the $C^+ + O^+$ fragmentation from CO at the C $1s \rightarrow \pi^*$ excitation. Solid curve: present data; dotted curve: Hitchcock *et al.* [24].

thors, with the exception of Lee *et al.*, are all higher than -0.90. These authors detected fragment ions with both low and high kinetic energies. Considering this fact, the kinetic-energy dependence of the β parameters would provide more information about these deviations. If the difference, however, is caused by the long lifetime of the core hole states, the β parameters may not depend on the kinetic energy of the fragment ions. If the difference originates from the long lifetime of the intermediate states before fragmentation, the β parameter may depend on the kinetic energy of the fragment ions because different intermediate states yield different kinetic energies.

Figure 4 shows the β parameters for the ionic fragmentation of $C^+ + O^+$ ion pairs for the excitations of C $1s$ to $2p\pi(\nu=0)$, $3s\sigma(\nu=0)$, and the σ^* shape resonance (photon energy of 305 eV) as a function of the total kinetic energy of $C^+ + O^+$. The values of the β parameter for the shown kinetic energies correspond to mean values of different kinetic energy ranges: 2 eV for 0–4 eV; 6 eV for 4–8 eV; 10 eV for 8–12 eV; 14 eV for 12–16 eV; 18 eV for 16–20 eV; 25 eV for 20–30 eV. The contributions from valence ionization to the β parameter are subtracted using the following equation [9]:

$$\beta_{\mathrm{exp}} = \beta_{\mathrm{C\ 1s}} \frac{\sigma_{\mathrm{C\ 1s}}}{\sigma_{\mathrm{C\ 1s}} + \sigma_{\mathrm{val}}} + \beta_{\mathrm{val}} \frac{\sigma_{\mathrm{val}}}{\sigma_{\mathrm{C\ 1s}} + \sigma_{\mathrm{val}}}, \qquad (5)$$

where β_{exp} is the experimentally determined angular distribution parameter, $\beta_{\mathrm{C\ 1s}}$ is the anisotropy parameter for electronic excitation involving only the C $1s$ electrons, β_{val} is the angular distribution parameter for valence ionization, $\sigma_{\mathrm{C\ 1s}}$ is the C $1s$ ion yield, and σ_{val} is the valence ion yield. The angular distribution parameter β_{val} was measured to be -0.04 at 285 eV below the $2p\pi$ excitation.

The β parameter for the $2p\pi$ excitation approaches -1 for increasing kinetic energies, which is the theoretically expected value. Likewise the β parameters for the $3s\sigma$ and σ^* excitations increase to 2 and 0.75, respectively, with increasing ion kinetic energies, as theoretically expected. The β parameter for the σ^* excitation is very close to the calculated maximum value of about 0.78 at 306.5 eV by Schirmer *et al.* [29] and about 0.75 by Lynch [30] based on the relaxed core Hartree-Fock method (RCHF) in contrast to the value of about 1.5 by Dehmer and Dill [14] based on the continuum multiple scattering method (CMSM). The experimental results suggest that only ion pairs with high kinetic energy

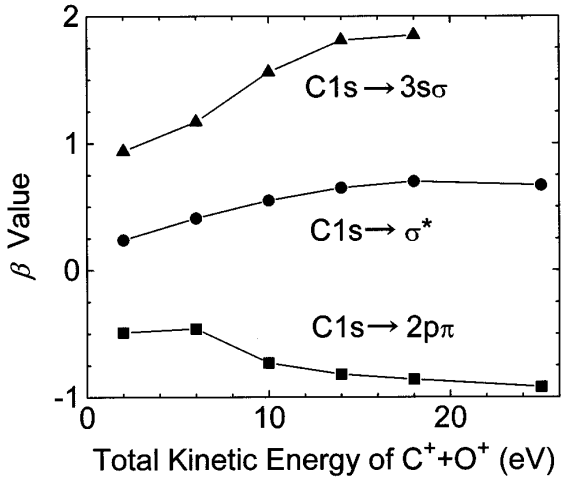

FIG. 4. Kinetic-energy dependence of the β parameter of $C^+ + O^+$ at the C $1s \rightarrow \pi^*$, $3s\sigma$, and σ^* excitations of CO.

provide information on the molecular orientation at the instant of the initial electronic excitation.

Previous measured β values by Hemmers *et al.* [8] at the π^* and the σ^* excitations are -0.95 and 0.7, respectively, which is very close to the present asymptotic values of -0.95 and 0.75, respectively. The reason for this agreement is that the previous study only detected fast ionic fragments to determine the anisotropy parameters. On the contrary, a relatively smaller β value, -0.79, was obtained by Bozek *et al.* [9]. This is because they detected fragment ions with all kinetic energies to determine the anisotropy parameter, resulting in lower effective β values.

If the potential curve is repulsive and proportional to $1/r$, where r is the internuclear distance between C and O atoms, the time scale of the fragmentation is much faster than the rotational motion at room temperature even though the kinetic-energy release is only 1 eV. A 10-Å separation between the C and O atoms then takes about 10^{-14} s and the β parameter is not affected by the different kinetic energies of the fragmentations. The intermediate states of CO^{2+} have a long lifetime and the potential curves for the fragmentation exhibit some stable features. However, for the fragmentation with high kinetic-energy release, the potential curve is similar to a simple repulsive curve and the β parameter reflects the molecular orientation at the initial photoabsorption. This is supported by the study of the potential curves for CO^{2+} calculated by Wetmore *et al.* [25]. The lower three potential curves of CO^{2+}, $^3\Pi$, $^1\Pi$, and $^1\Sigma^+ - 1$, with the binding energies (BE) of 41.0, 41.6, and 41.9 eV, respectively, at the equilibrium geometry of ground-state CO, have a minimum in the Franck-Condon region (i.e., at $1.08 < R < 1.18$ Å), indicating that CO^{2+} is stable until it dissociates through a tunnel effect or predissociation. The dissociation energies of $C^+ + O^+$ from CO^{2+} in the $^3\Pi$, $^1\Pi$, and $^1\Sigma^+ - 1$ are 5.0, 2.3, and 2.7 eV, respectively [24]. The next potential curve $^3\Sigma^-$ (BE of 43.4 eV) has no minimum in the Franck-Condon region, but there is a minimum at a larger internuclear distance. This potential curve yields a kinetic energy of 7.4 eV for $C^+ + O^+$. The potential curves of $^1\Sigma^+ - 2$ (BE of 48.4 eV) and $^1\Delta$ (BE of 47.0 eV), which produce kinetic energies of 7.4 and 7.7 eV, respectively, have a smaller minimum but are relatively constant at internuclear distances

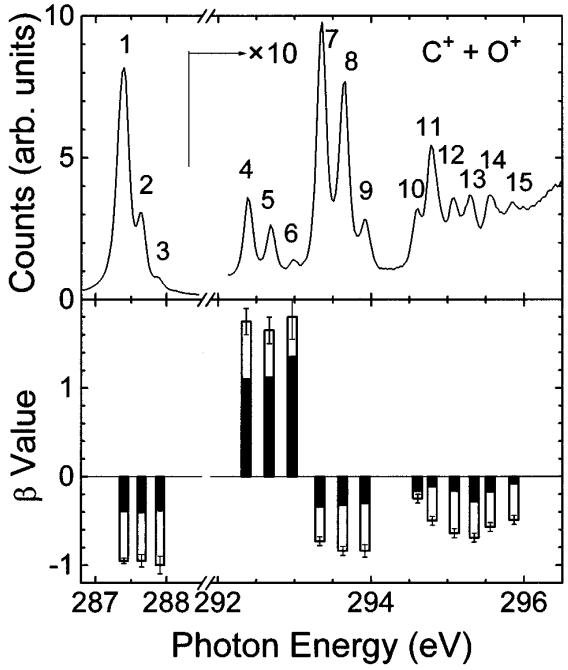

FIG. 5. β parameters of the $C^+ + O^+$ fragmentations from C $1s \rightarrow nl\lambda$ excited CO derived from the high kinetic-energy data (more than 12 eV, the open bars with error bars) and from the low kinetic-energy data (4–8 eV, solid bars).

larger than 1.5 Å . The potential curves of $^3\Sigma^+$ (BE of 48.7 eV) and $^3\Delta$ (BE of 49.9 eV), which release kinetic energies of 9.4 and 10.6 eV, have a small minimum in the Franck-Condon region but outside a repulsive-type potential curve. The molecular ion, CO^{2+}, would dissociate faster along these potential curves than in the former potential curves. The potential curves of $^1\Sigma^+$ (BE of 58.6 eV) and $^1\Sigma^+$ (BE of 60.4 eV), resulting in a high kinetic-energy release of $C^+ + O^+$, 17.6 and 19.1 eV, respectively, behave like a $1/r$ curve. This suggests that the time scale of fragmentation is very fast. Fragmentation of $C^+ + O^+$ with low kinetic-energy release cannot take place directly along the potential curves. This means that the ion pairs are produced through predissociation or tunneling between the potential curves. These processes last so long that the molecular axis starts to rotate in the mean time. Therefore, the β values measured are lower than those expected from the symmetry transitions. The ion pairs with high kinetic energies are generated directly along the repulsive potential curves. In this case the process does not last long enough to make it possible for the molecular axis to rotate, yielding β values which reflect the orientation of the molecular bond axis at the instant of the initial electronic excitation.

V. ANGULAR DISTRIBUTIONS OF $C^+ + O^+$ IN THE C 1s EXCITATION REGION

Figure 5 shows the anisotropy parameters β of the $C^+ + O^+$ fragmentation in the C $1s$ excitation region with vibrationally resolved core levels, and the ion yield spectrum of $C^+ + O^+$. In order to determine the symmetry of the C $1s$ excited states, the data with a kinetic energy of more than 12 eV was used (open bars with error bars). The measured

TABLE II. The β parameter of CO in C $1s$ excitation region with assignments by Domke *et al.* [16].

Label	Energy (eV)	Assignments [16]	β value
1	287.40	$1s^{-1}2p\pi(\nu=0)$	−0.95
2	287.65	$1s^{-1}2p\pi(\nu=1)$	−0.95
3	287.91	$1s^{-1}2p\pi(\nu=2)$	−1.0
4	292.37	$1s^{-1}3s\sigma(\nu=0)$	1.75
5	292.67	$1s^{-1}3s\sigma(\nu=1)$	1.65
6	292.97	$1s^{-1}3s\sigma(\nu=2)$	1.8
7	293.33	$1s^{-1}3p\pi(\nu=0)$	−0.73
	293.50	$1s^{-1}3p\sigma(\nu=0)$	
8	293.63	$1s^{-1}3p\pi(\nu=1)$	−0.84
	293.80	$1s^{-1}3p\sigma(\nu=1)$	
9	293.92	$1s^{-1}3p\pi(\nu=2)$	−0.84
10	294.61	$1s^{-1}3d\pi(\nu=0)$	−0.25
11	294.80	$1s^{-1}4p\pi(\nu=0)$	−0.50
	294.92	$1s^{-1}3d\pi(\nu=1)$	
12	295.09	$1s^{-1}4p\pi(\nu=1)$	−0.64
	295.23	$1s^{-1}3d\pi(\nu=2)$	
	295.27	$1s^{-1}4d\pi(\nu=0)$	
13	295.35	$1s^{-1}5p\pi(\nu=0)$	−0.69
	295.37	$1s^{-1}4p\pi(\nu=2)$	
	295.56	$1s^{-1}4d\pi(\nu=1)$	
14	295.56	$1s^{-1}6p\pi(\nu=0)$	−0.57
	295.65	$1s^{-1}5p\pi(\nu=1)$	
	295.74	$1s^{-1}7p\pi(\nu=0)$	
15	295.87	$1s^{-1}6p\pi(\nu=1)$	−0.49

β values with the higher kinetic energies reflect the intrinsic symmetry of the excited states as described in the previous section. The contribution from valence ionization to the β parameter values is subtracted using Eq. (5). Table II shows the β parameter, together with the assignments of the excited states [16]. We show in addition the β values derived from the low kinetic-energy data (4–8 eV, solid bars in Fig. 5) which are significantly lower but mimic the high-energy behavior for most of the vibrational progressions. Possible variations between the behavior of the two sets of data may be seen for lines above 294 eV. These lines, however, are not suited for an examination of the angular behavior with respect to vibrational effects because they belong to different vibrational series.

Three vibrational levels ($\nu=0,1,2$) are seen for $2p\pi$, $3s\sigma$, and $3p\pi$. At the $2p\pi$ excitation, all the β values are close to -1, which is the expected value for the transition of Σ to Π. The vibrational levels do not affect the anisotropy parameter. At the $3s\sigma$ excitation, the β values are around 1.7, which is close to the expected value of 2 for the transition of Σ to Π. The β values for $3s\sigma$ do not depend on the vibrational levels. At the $3p\pi$ excitation, all the β values are around -0.85, which is higher than the expected value of -1 for the excitation of Σ to Π. It is reported that $3p\sigma$ states exist between $3p\pi$ states [16]. If the contribution of $3p\sigma$ is 5% of the total intensity, the β value becomes -0.85. The β values of the excitations $2p\pi$, $3s\sigma$, and $3p\pi$ show also that the vibrational levels do not affect the anisotropy parameter.

For the excitations to Rydberg orbitals, all the β values

are negative. The β value is -0.25 for peak 10 and decreases to -0.69 at peak 13 and increases to -0.49 for the peak 15. Since the assignments in this region are all π-type excitations, the β values in this region should be -1. There is also a contribution of the continuum ionization in this Rydberg region. The transitions of the continuum ionization have both σ and π symmetries. The increase of the β value, -0.69, for peak 13 to -0.49 for peak 15 may come from the contribution of the C $1s$ continuum ionization. This cross section of the C $1s$ continuum ionization increases when the photon energy approaches the C $1s$ ionization threshold. However, continuum ionization is not the cause for the lower β values of peaks 10–12. A transition of σ symmetry must exist in order to explain the present result. The β values of the excitations to $3p\pi$ and $3d\pi$ obtained by Bozek *et al.* [19] are -0.46 and -0.27, respectively. Since the photon-energy resolution was not high enough in this experiment, the β values are lower than the intrinsic values. However, the β value at $3d\pi$ is higher than that at $3p\pi$, suggesting that a σ symmetry transition exists around the peak $3d\pi$. The symmetry-resolved ion yield spectra of CO measured by Shigemasa *et al.* [7] show a contribution of a σ-type excitation in this region. Our previous high-resolution study [20] reported that the excitations to $4s\sigma$ states in the CO^+ ion yield curve exist. These $4s\sigma$ states are located close to the transitions to $3d\pi$ and $4p\pi$. Therefore, the contribution of the $4s\sigma$ excitations lower the β values for peaks 10–12.

VI. SUMMARY

The angular distributions for the fragmentation of $C^+ + O^+$ were measured with core vibrational resolution using an angle-resolved TOF mass spectrometer, which has a multihit position-sensitive anode. The β parameter approaches theoretically expected intrinsic value with increasing kinetic energy of the fragmentation pair. This suggests that the corresponding potential curves of the Auger final states have stable features at lower fragmentation energies. The anisotropy parameter in the C $1s$ excitation region was determined with core vibrational resolution. The core vibration does not affect the β parameter. The excitation of C $1s$ to $4s\sigma$ lies near the $3d\pi$ and $4p\pi$ excitations.

ACKNOWLEDGMENTS

This research was funded by the Bundesminister für Bildung, Wissenschaft, Forschung und Technologie (BMBF) and by the Deutsche Forschungsgemeinschaft. N.S. is grateful to the Alexander von Humboldt Foundation for financial support. F.H. acknowledges financial support by the Deutscher Akademischer Austauschdienst.

[1] A. P. Hitchcock, J. Electron Spectrosc. Relat. Phenom. **25**, 245 (1982).
[2] N. Saito and I. H. Suzuki, Phys. Rev. Lett. **61**, 2740 (1989).
[3] N. Saito and I. H. Suzuki, J. Phys. B **22**, 3937 (1989).
[4] A. Yagishita, H. Maezawa, M. Ukai, and E. Shigemasa, Phys. Rev. Lett. **62**, 36 (1989).
[5] E. Shigemasa, K. Ueda, Y. Sato, T. Hayaishi, H. Maezawa, T. Sasaki, and A. Yagishita, Phys. Scr. **41**, 63 (1990).
[6] K. Lee, D. Y. Kim, I. Ma, D. A. Lapiano-Smith, and D. A. Hanson, J. Chem. Phys. **93**, 7936 (1990).
[7] E. Shigemasa, T. Hayaishi, T. Sasaki, and A. Yagishita, Phys. Rev. A **47**, 1824 (1993).
[8] O. Hemmers, F. Heiser, J. Eiben, R. Wehlitz, and U. Becker, Phys. Rev. Lett. **71**, 987 (1993).
[9] J. D. Bozek, N. Saito, and I. H. Suzuki, J. Chem. Phys. **100**, 393 (1994).
[10] N. Saito and I. H. Suzuki, J. Phys. B **22**, L517 (1989).
[11] N. Kosugi, E. Shigemasa, and A. Yagishita, Chem. Phys. Lett. **190**, 481 (1992).
[12] N. Saito and I. H. Suzuki, Phys. Rev. A **43**, 3662 (1991).
[13] N. Kosugi, J. Adachi, E. Shigemasa, and A. Yagishita, J. Chem. Phys. **97**, 8842 (1993).
[14] J. L. Dehmer and D. Dill, Phys. Rev. Lett. **35**, 213 (1975).
[15] C. T. Chen, Nucl. Instrum. Methods A **256**, 595 (1987); C. T. Chen and F. Sette, Rev. Sci. Instrum. **60**, 1616 (1989).
[16] M. Domke, C. Xue, A. Puschmann, T. Mandel, E. Hudson, D. A. Shirley, and G. Kaindl, Chem. Phys. Lett. **173**, 122 (1990); **174**, 668(E) (1990).
[17] K. J. Randall, A. L. D. Kilcoyne, H. M. Köppe, J. Feldhaus, A. M. Bradshaw, J.-E. Rubensson, W. Eberhardt, Z. Xu, P. D. Johnson, and Y. Ma, Phys. Rev. Lett. **71**, 1156 (1993).
[18] C. T. Chen, Y. Ma, and F. Sette, Phys. Rev. A **40**, 6737 (1989).
[19] K. Lee, D. Y. Kim, C.-I. Ma, and D. M. Hanson, J. Chem. Phys. **100**, 8550 (1994).
[20] N. Saito, F. Heiser, O. Hemmers, A. Hempelmann, K. Wieliczek, J. Viefhaus, and U. Becker, Phys. Rev. A **51**, R4313 (1995).
[21] A. R. B. de Castro and R. Reininger, Rev. Sci. Instrum. **63**, 1317 (1992); C. U. S. Larsson, A. Beutler, O. Björneholm, F. Federmann, U. Hahn, A. Rieck, S. Verbin, and T. Möller, Nucl. Instrum. Methods A **337**, 603 (1994).
[22] F. Heiser, K. Wieliczek, N. Saito, and U. Becker (unpublished).
[23] H. Heins and L. Karlsson, *Photoelectron Spectroscopy*, Handbuch der Physik Vol. 31, edited by S. Flügge and W. Mehlhorn (Springer-Verlag, Berlin, 1982).
[24] A. P. Hitchcock, P. Lablanquie, P. Morin, E. Lizon, A. Lugrin, M. Simon, P. Thiry, and I. Nenner, Phys. Rev. A **37**, 2448 (1988).
[25] R. W. Wetmore, R. J. Le Roy, and R. K. Boyd, J. Phys. Chem. **88**, 6318 (1984).
[26] N. Correia, A. Flores-Rivers, H. Ågren, K. Helenelnd, L. Asplund, and U. Gelius, J. Chem. Phys. **83**, 2035 (1985).
[27] A. Flores-Rivers, N. Correia, H. Ågren, L. Petterson, M. Bäckström, and J. Nordgren, J. Chem. Phys. **83**, 2053 (1985).
[28] G. Herzberg, *Molecular Spectra and Molecular Structure* (Van Nostrand, New York, 1950), Vol. 1.
[29] J. Schirmer, M. Braunstein, and V. McKoy, Phys. Rev. A **41**, 283 (1990).
[30] D. L. Lynch, Phys. Rev. A **43**, 5176 (1991).